Yang et al. Journal of Analytical Science and Technology (2016) 7:9
DOI 10.1186/s40543-016-0089-2

Journal of Analytical Science and Technology
a SpringerOpen Journal

SHORT REPORT Open Access

Spectroscopic determination of alkyl resorcinol concentration in hydroxyapatite composite

Won-Geun Yang[1], Jeong-Hyon Ha[2], Seong-Gon Kim[3] and Weon-Sik Chae[1*]

Abstract

Background: Recently, alkyl resorcinol compounds showed remarkable improvements on dental implant restoration as well as anaesthetic, antiseptic, and anthelmintic applications. In this study, we prepared biologically functional composition of 4-hexylresorcinol (4HR)-loaded hydroxyapatite (HA).

Findings: Attenuated total reflectance (ATR) Fourier-transform infrared (FT-IR) spectroscopy fully assigned vibrational absorptions of 4-hexylresorcinol as well as the HA. The absorption coefficient of 4HR aqueous solution is estimated to be 1393 ± 61 cm^{-1} M^{-1} at highly diluted concentration. The 4HR was loaded with 0.018 % (wt/wt) in the 4HR-HA composite.

Conclusions: We quantitatively determined the micromolar concentration of 4HR loaded in the composite based on ultraviolet-visible (UV-Vis) absorption spectroscopy.

Keywords: 4-hexylresorcinol, Hydroxyapatite, ATR-FT-IR, UV-Vis

Findings

Background

Hydroxyapatite (HA) is the major component of bone material and a hexagonally packed crystal with hydroxyl end members (Pleshko et al. 1991). HA analogue materials have been extensively developed through a variety of chemical and physical routes (Ferraz et al. 2004; Bouyer et al. 2000; Cengiz et al. 2008). One of tremendous use of HA is bone grafting application via coating metallic dental implant surface, which stimulates bone healing and therefore improves implant integration rate and strength (Cook et al. 1987; Lange and Donath 1989). According to previous reports, however, HA-coated dental implants have often failed because of bacterial infection (Chang and Tanaka 2002; Destainville et al. 2003; Coates 2000). Hence, infection-resistant HA coating with bioinert antiseptic function is of great interest. Recently, a 4-hexylresorcinol (4HR)-treated HA-titanium dental implant showed significant improvement in both bone formation and bone-to-implant contact after implant surgery (Kim et al. 2011a).

Alkyl resorcinols, natural non-isoprenoid phenolic lipids found in plants (Tyman 1979), have attracted much attention due to a variety of biologic functions, such as being nonspecific antioxidants, antimutagens, and regulatory molecules (Kim et al. 2011b). Hexylresorcinol is an organic compound with well-known anaesthetic, antiseptic, and anthelmintic properties (Wilson and Gisvold 1954). By now, hexylresorcinol have been used in a variety of application areas, such as skincare products with anti-aging function, food additive with estrogenic activity (Amadasi et al. 2009), and anti-cancer activity by inhibiting NF-κB (Kim et al. 2011a). Hexylresorcinol inhibits the formation of graft-induced foreign body giant cells (Kweon et al. 2014). Therefore, hexylresorcinol has been used for bone substitute-related tissue engineering (Lee et al. 2015).

Several routes have been tried to deposit 4HR on the hydrophilic HA; however, precise control of 4HR loading amount is still challenging because of the amphiphilic character of 4HR (Kim et al. 2011b). Therefore, quantitative determination of the loading amount is importantly required to further optimize

* Correspondence: wschae@kbsi.re.kr
[1]Analysis Research Division, Daegu Center, Korea Basic Science Institute, Daegu 41566, Republic of Korea
Full list of author information is available at the end of the article

composite materials with a demanded function (Kweon et al. 2014; Lee et al. 2015). In this study, solution-processed 4HR-loaded HA composite were quantitatively characterized using Fourier-transform infrared (FT-IR) and ultraviolet-visible (UV-Vis) absorption spectroscopies. Infinitesimal amount of 4HR, which was loaded on HA powder, could be detected and precisely estimated based on UV-Vis absorption spectroscopy. Additionally, we entirely assigned IR absorption peaks of 4HR for the first time.

Material and methods

Chemicals and materials

Hydroxyapatite (reagent grade) and 4-hexylresorcinol (98 %) were used as received from Sigma Aldrich. 4HR-loaded HA composite (4HR-HA) was prepared in aqueous medium for FT-IR and UV-Vis absorption study. 0.5 g of hydroxyapatite was mixed with 50 ml of 0.1 M 4-hexylresorcinol aqueous solution and then stirred at 200 rpm for 1 h. The suspension was finally filtered and dried for 24 h.

Spectroscopic characterization

FT-IR absorption spectra were obtained using a Fourier-transform spectrometer (Vertex 80, Bruker Optics) equipped with an attenuated total reflectance (ATR) accessory (MIRacle, PIKE technologies). Spectrum was recorded in the spectral range of 600 to 4000 cm^{-1} at a resolution of 2 cm^{-1} with a mercury cadmium telluride detectors (MCT detector), and 128 repeated scans were averaged for each spectrum. The UV-Vis absorption spectra were obtained using a spectrophotometer (S-3100, Scinco).

Results and discussion

We performed FT-IR absorption study to evaluate the loading amount of 4HR in HA composite powder. Figure 1 shows IR absorption spectrum of the bare HA powder, which presented the phosphate band between 900 and 1200 cm^{-1}. In Fig. 1, there are PO_4^{3-} ν_1 mode at 962 cm^{-1} (Chang and Tanaka 2002; Kim et al. 2011a; Han et al. 2006) and PO_4^{3-} ν_3 mode at 1028 (Chang and Raynaud et al. 2002; Destainville et al. 2003; Kim et al. 2011b; Han et al. 2006; Kim et al. 2012), 1088 (Chang and Raynaud et al. 2002; Destainville et al. 2003; Kim et al. 2011a; Han et al. 2006; Kim et al. 2012), and 870 cm^{-1} (Destainville et al. 2003; Han et al. 2006) band for HPO_4^{3-} and labile PO_4^{3-} mode at 632 cm^{-1} (Chang and Tanaka 2002; Kim et al. 2011b). Adsorbed water shows relatively wide stretching vibrational absorption in mid-IR region from 3600 to 3000 cm^{-1} with a distinct peak at 3572 cm^{-1}. The absorption peak observed at 3572 cm^{-1} indicates the presence of the –OH group (Kim et al. 2011a; Raynaud et al. 2002; Han et al. 2006; Kim et al. 2012). Summarized data are shown in Table 1.

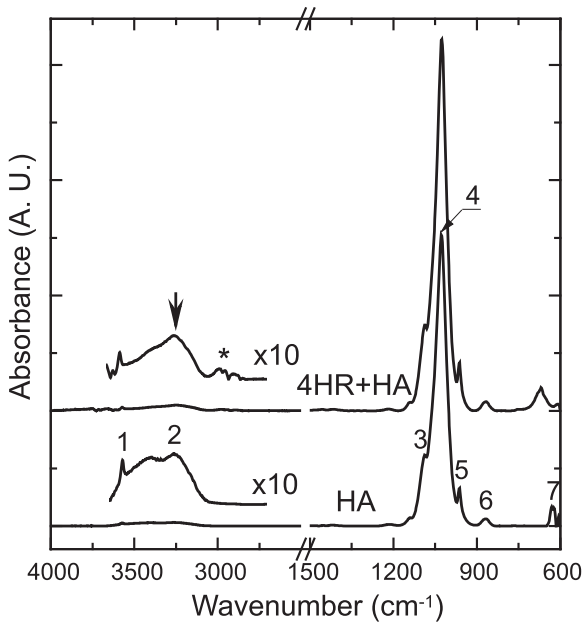

Fig. 1 FT-IR absorption spectra of the HA and the 4HR-loaded HA

Figure 2 shows the FT-IR absorption spectrum of 4-hexylresorcinol. The vibrational absorption peak at 3039 cm^{-1} corresponds to the aromatic hydrocarbon, and the absorbance peaks at 3340 and 3419 cm^{-1} are assigned to hydrogen bonding between hydroxyl groups in benzene ring (Kim et al. 2012). The characteristic C–H stretching vibrations for saturated aliphatic species occur between 3000 and 2800 cm^{-1}, and the corresponding simple bending vibrations nominally occur between 1500 and 1300 cm^{-1}. The absorption peaks at 2960, 2922, 2873, and 2856 cm^{-1} are corresponding to the well-known asymmetric and

Table 1 Characteristic IR absorptions of hydroxyapatite

Wavenumber (cm^{-1})	Bond	Position	Reference
3572	OH^-	1	(Kim et al. 2011a; Raynaud et al. 2002; Han et al. 2006; Kim et al. 2012)
3000~3600	H_2O	2	(Meejoo et al. 2006)
1028, 1088	PO_4^{3-} (v3)	3, 4	(Chang & Raynaud et al. 2002; Destainville et al. 2003; Kim et al. 2011b; Han et al. 2006; Kim et al. 2012)
962	PO_4^{3-} (v1)	5	(Chang and Tanaka 2002; Kim et al. 2011a; Han et al. 2006)
870	HPO_4^{3-}	6	(Destainville et al. 2003; Han et al. 2006)
632	Labile PO_4^{3-}	7	(Chang and Tanaka 2002; Kim et al. 2011b)

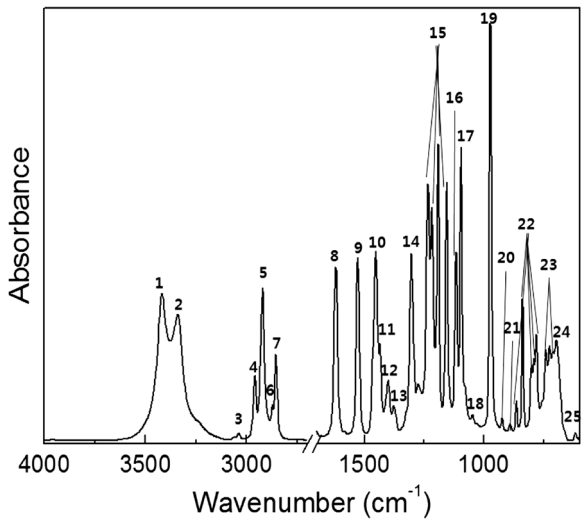

Fig. 2 FT-IR absorption spectrum of 4-hexylresocinol

symmetric stretching modes of aliphatic hydrocarbons (Coates 2000; Kim et al. 2011b; Kim et al. 2012; Krimm et al. 1956). Aromatic ring stretching vibration was observed at 1620 and 1527 cm^{-1} (Coates 2000). The absorption at 1452 cm^{-1} and the two weak peaks at 1435 and 1377 cm^{-1} are corresponding to the bending mode and the asymmetric and symmetric stretching modes of the aliphatic hydrocarbons, respectively (Coates 2000; Krimm et al. 1956). The phenolic OH bending mode of phenol species occurs at 1398 cm^{-1} (Coates 2000). The absorption peak at 1304 cm^{-1} reveals aliphatic CH_2 wagging mode in disordered phase (Krimm et al. 1956). The intense absorptions at 1234, 1217, 1192, 1155, and 924 cm^{-1} are responsible for the C–O stretching modes in phenol species (Silverstein et al. 1991; Choo et al. 2011). The absorption peak at 1116 cm^{-1} can be assigned to the C–C–H bending mode (Cui et al. 2013). The absorption peaks at 1095, 974, 891 and 740, and 725 cm^{-1} were assigned to the C–C stretching mode (Krimm et al. 1956; Gómez-Sánchez et al. 2011), the CH_2 wagging or twisting mode (Hallos 1984), the CH_3 rocking mode (Krimm et al. 1956), and the CH_2 rocking mode (Coates 2000; Krimm et al. 1956) of

Table 2 Characteristic IR absorptions of 4-hexylresorcinol

Wavenumber (cm^{-1})	Bond	Position	Reference
3340, 3419	Hydrogen bonded OH stretching	1, 2	(Kim et al. 2012)
3039	Aromatic CH stretching	3	(Kim et al. 2012)
2960	Aliphatic CH_3 asymmetric stretching	4	(Coates 2000; Kim et al. 2012)
2922	Aliphatic CH_2 asymmetric stretching	5	(Coates 2000; Kim et al. 2011a; Kim et al. 2012)
2873	Aliphatic CH_3 symmetric stretching	6	(Coates 2000; Kim et al. 2012)
2856	Aliphatic CH_2 symmetric stretching	7	(Coates 2000; Kim et al. 2011b; Kim et al. 2012)
1620, 1527	Aromatic ring C–C stretching	8, 9	(Coates 2000)
1452	Aliphatic CH_2 bending	10	(Coates 2000; Krimm et al. 1956)
1435	Aliphatic CH_3 asymmetric bending	11	(Coates 2000)
1398	Phenolic OH bending	12	(Coates 2000)
1377	Aliphatic CH_3 symmetric bending	13	(Coates 2000; Krimm et al. 1956)
1304	Aliphatic CH_2 wagging (disordered phase)	14	(Krimm et al. 1956)
1234, 1217, 1192, 1155	C–O stretching	15	(Silverstein et al. 1991; Choo et al. 2011)
1116	C–C–H bending	16	(Hallos 1984)
1095	C–C stretching	17	(Krimm et al. 1956; Frost et al. 2007)
1047	OH deformation stretching	18	(Evanoff and Chumanov 2004)
974	CH_2 wagging or twisting	19	(Kozubek and Tyman 1999)
924	C–O stretching	20	(Cui et al. 2013; Gómez-Sánchez et al. 2011)
891	CH_3 rocking	21	(Krimm et al. 1956)
864, 839, 800, 791, 779	Aromatic C–H out-of-plane bending	22	(Coates 2000; Silverstein et al. 1991)
725, 740	CH_2 rocking	23	(Coates 2000; Krimm et al. 1956)
696	Out-of-plane ring C=C bending	24	(Silverstein et al. 1991)
617	OH out-of-plane bending	25	(Silverstein et al. 1991)

aliphatic hydrocarbons, respectively. The absorption peaks at 1047 cm^{-1} are for the OH deformation stretching mode (Frost et al. 2007). The IR absorption peaks at 864, 839, 800, 791, and 779 cm^{-1} can be assigned to the aromatic C–H out-of-plane bending mode (Coates 2000; Silverstein et al. 1991). The peaks at 696 and 617 cm^{-1} are assigned to the out-of-plane ring C=C bending and OH out-of-plane bending modes, respectively (Silverstein et al. 1991). Detailed assignments are fully summarized in Table 2.

FT-IR spectrum of the 4HR-HA composite showed the majority absorptions for the HA without any distinct change (Fig. 1). Additionally, very weak C–H stretching absorption corresponding to the 4HR is observed in the region of 2800–3000 cm^{-1} (asterisk indicated). After 4-hexylresorcinol treatment, the 4HR-HA composite showed enhanced absorption at 3260 cm^{-1} (arrow indicated). This can be attributed to hydrogen bonding between 4HR and HA. However, it is still ambiguous to precisely estimate 4HR concentration in this composite.

From the absorption spectrum in the UV-Vis region (Fig. 3), the 4HR aqueous solution showed the characteristic absorption at ~270 nm, corresponding to π–π* electronic transition (Silverstein et al. 1991). As a function of concentration, absorption coefficient value is decreased (inset of Fig. 3a). According to the previous reports, alkyl resorcinols with a long hydrocarbon tail easily tend to aggregate to form micelles in an aqueous medium (Kozubek and Tyman 1999), hence, inevitably reducing absorption efficiency. Therefore, the absorption coefficient of 4HR aqueous solution is estimated at a highly diluted concentration, which enabled the absorption coefficient of 1393 ± 61 cm^{-1} M^{-1}.

The additional absorption was also shown at ~430 nm, which is attributed to the scattering of HA powder. A colloidal powder suspension typically scatters light in the visible region. The scattering absorption can vary as a function of colloidal particle size (Evanoff and Chumanov 2004; Chae et al. 2009). In this study, the bulk HA powder showed a broad scattering with a maximum at 535 nm. As the HA was treated with 4HR, the scattering peak was observed at 430 nm. This blue-shifted scattering seems to be attributed to the fragmentation of the HA powder after 4HR treatment.

It is noteworthy that the absorption spectrum of the 4HR-loaded HA powder clearly reveals the presence of 4HA. The measured absorbance of 0.0065 is corresponding to 4.7 μM concentration and 3.5 μg 4HR in a standard cuvette. Regarding the total 4HR-HA composite powder mass of 19 mg for the UV-Vis measurement, the 4HR was loaded with 0.018 % (wt/wt) in the 4HR-HA composite. This small loading amount reasonably explains why IR spectroscopy need to take extra special care on sampling to determine the 4HR concentration even in ATR mode with a typical detection limit of ~0.1 wt % or 10^{-4} M.

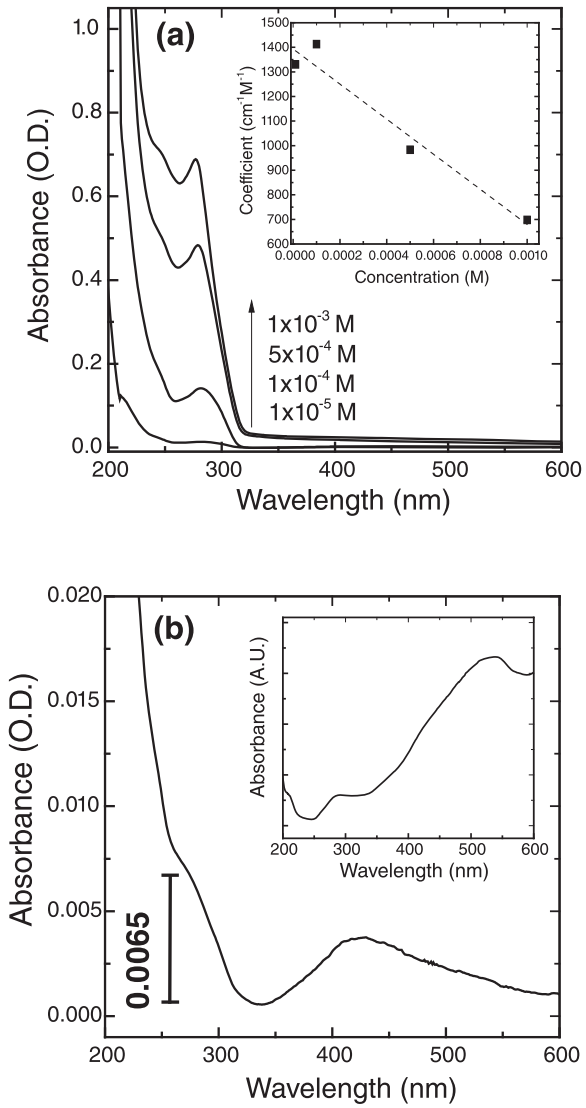

Fig. 3 UV-Vis absorption spectra of the 4HR (**a**) and the 4HR-loaded HA composite powder (**b**). *Inset* of **a** is the absorption coefficients of 4HR as a function of concentration. *Inset* of **b** is the absorption spectrum of the HA powder aqueous mixture (5 mg/ml)

Conclusions

We estimated an amount of 4-hexylresorcinol compound from its composite form with hydroxyapatite using FT-IR and UV-Vis absorption spectroscopies. Because of the majority IR absorptions of HA, the precise estimation of 4HR concentration in the 4HR-HA composite is a little ambiguous using FT-IR spectroscopy. On the other hand, the 4HR-HA composite showed

clear absorption for 4HR in the ultraviolet region. Based on UV-Vis absorption spectroscopy, we effectively estimated the micromolar quantity of the loaded 4HR in the 4HR-HA composite.

Competing interests
All authors declare that they have no competing interests.

Authors' contributions
WSC designed the study. WGY and WSC performed research. WGY and JHH carried out FT-IR analysis. WGY and WSC carried out UV-Vis absorption analysis. WGY, SGK, and WSC wrote the manuscript. All authors read and approved the final manuscript.

Acknowledgements
This research was supported by Basic Science Research Program through the National Research Foundation of Korea (NRF) funded by the Ministry of Education (NRF-2015R1D1A1A01058935).

Author details
[1]Analysis Research Division, Daegu Center, Korea Basic Science Institute, Daegu 41566, Republic of Korea. [2]Space-Time Resolved Molecular Imaging Research Team, Korea Basic Science Institute, Seoul 02855, Republic of Korea. [3]Department of Oral and Maxillofacial Surgery, College of Dentistry, Gangneung-Wonju National University, Gangneung 25457, Republic of Korea.

Received: 4 February 2016 Accepted: 8 March 2016
Published online: 14 March 2016

References
Amadasi A, Mozzarelli A, Meda C, Maggi A, Cozzini P. Identification of xenoestrogens in food additives by an integrated in silico and in vitro approach. Chem Res Toxicol. 2009;22:52–63.
Bouyer E, Gitzhofer F, Boulos MI. Morphological study of hydroxyapatite nanocrystal suspension. J Mater Sci: Mater Med. 2000;11:523–31.
Cengiz B, Gokce Y, Yildiz N, Aktas Z, Calimli A. Synthesis and characterization of hydroxyapatite nanoparticle. Colloids Surf A: Physicochem Eng Aspects. 2008; 322:29–33.
Chae WS, Kershner RJ, Braun PV. Fabrication of 50 to 1000 nm monodisperse ZnS colloids. Bull Korean Chem Soc. 2009;30:129–32.
Chang MC, Tanaka JZ. FT-IR study for hydroxyapatite/collagen nanocomposite cross-linked by glutaraldehyde. Biomater. 2002;23:4811–8.
Choo ESG, Tang XS, Sheng Y, Shuter B, Xue JM. Controlled loading of superparamagnetic nanoparticles in fluorescent nanogels as effective T2-weighted MRI contrast agents. J Mater Chem. 2011;21:2310–9.
Coates J. In Encyclopedia of Analytical Chemistry, Interpretation of Infrared Spectra, A Practical Approach. Chichester: John Wiley & Sons; 2000.
Cook SD, Kay JF, Thomas KA. Interface mechanics and histology of titanium and HA-coated titanium for dental implant applications. Int J Oral Maxillofac Implants. 1987;2:15–22.
Cui CZ, Park DH, Kim JY, Joo JS, Ahn DJ. Oligonucleotide assisted light-emitting Alq3 microrods: energy transfer effect with fluorescent dyes. Chem Commun. 2013;49:5360–2.
Destainville A, Champion E, Bernache-Assollant D, Laborde E. Synthesis, characterization and thermal behavior of apatitic tricalcium phosphate. Mater Chem Phys. 2003;80:269–77.
Evanoff DD, Chumanov G. Size-controlled synthesis of nanoparticles. 2. Measurement of extinction, scattering, and absorption cross sections. J Phys Chem B. 2004;108:13957–62.
Ferraz MP, Monteiro FJ, Manuel CM. Hydroxyapatite nanoparticles: a review of preparation methodologies. J Appl Biomater Biomech. 2004;2:74–80.
Frost RL, Wain DL, Martens WN, Reddy BJ. Vibrational spectroscopy of selected minerals of the rosasite group. Spectrochim Acta Part A: Mol Biomol Spectrosc. 2007;66:1068–74.
Gómez-Sánchez E, Simon S, Koch LC, Wiedmann A, Weber T, Mengel M. ATR-FTIR spectroscopy for the characterization of magnetic tape materials. e-Preserv Sci. 2011;8:2–9.
Hallos RS. A "chain fold band" in the infrared spectra of nylon 6. J Appl Polym Sci. 1984;29:3907–14.
Han JK, Song HY, Saito FM, Lee BT. Synthesis of high purity nano-sized hydroxyapatite powder by microwave-hydrothermal method. Mater Chem Phys. 2006;99:235–9.
Kim SG, Hahn BD, Park DS, Lee YC, Choi EJ, Chae WS, et al. Aerosol deposition of hydroxyapatite and 4-hexylresorcinol coatings on titanium alloys for dental implants. J Oral Maxillofac Surg. 2011a;69:354–63.
Kim SG, Lee SW, Park YW, Jeong JH, Choi JY. 4-hexylresorcinol inhibits NF-κB phosphorylation and has a synergistic effect with cisplatin in KB cells. Oncol Rep. 2011b;26:1527–32.
Kim MK, Park YT, Kim SG, Park YW, Lee SK, Choi WS. The effect of a hydroxyapatite and 4-hexylresorcinol combination graft on bone regeneration in the rabbit calvarial defect model. Korean Assoc Maxillofac Plast Reconstr Surg. 2012;34: 377–83.
Kozubek A, Tyman JHP. Resorcinolic lipids, the natural non-isoprenoid phenolic amphiphiles and their biological activity. Chem Rev. 1999;99:1–25.
Krimm SCYL, Liang CY, Sutherland GBBM. Infrared spectra of high polymers. II. Polyethylene. J Chem Phys. 1956;25:549–62.
Kweon H, Kim SG, Choi JY. Inhibition of foreign body giant cell formation by 4-hexylresorcinol through suppression of diacylglycerol kinase delta gene expression. Biomater. 2014;35:8576–84.
Lange GL, Donath K. Interface between bone tissue and implants of solid hydroxyapatite or hydroxyapatite-coated titanium implants. Biomater. 1989;10:121–5.
Lee SW, Um IC, Kim SG, Cha MS. Evaluation of bone formation and membrane degradation in guided bone regeneration using a 4-hexylresorcinol-incorporated silk fabric membrane. Maxillofac Plast Reconstr Surg. 2015;37:32–6.
Meejoo S, Maneeprakorn W, Winotai P. Phase and thermal stability of nanocrystalline hydroxyapatite prepared via microwave heating. Thermochim Acta. 2006;447:115–20.
Pleshko N, Boskey A, Mendelsohn R. Novel infrared spectroscopic method for the determination of crystallinity of hydroxyapatite minerals. Biophys J. 1991;60: 786–93.
Raynaud S, Champion E, Bernache-Assollant D, Thomas P. Calcium phosphate apatites with variable Ca/P atomic ratio I. Synthesis, characterisation and thermal stability of powders. Biomater. 2002;23:1065–72.
Silverstein RM, Bassler GC, Morrill TC. In Spectrometric identification of organic compounds, Infrared Spectrometry. New York: John Wiley & Sons; 1991
Tyman JHP. Non-isoprenoid long chain phenols. Chem Soc Rev. 1979;8:499–537.
Wilson CO, Gisvold O. Textbook of organic medicinal and pharmaceutical chemistry. Philadelphia: Lippincott; 1954. 237-262